Corrosion of SS316H in Static and Flowing U-Bearing Fluoride Salt

10/30/2023

Ph.D. Student: Jaewoo Park

Advisor: Jinsuo Zhang

VIRGINIA TECH

Molten salt corrosion is impurity-driven

- Non-Metal impurities

  Examples: H_2O, O_2, HF, HCl, S^{2-}, O^{2-},H^{+}

- Metal impurities:

  Examples: Fe^{2+}, Ni^{2+}, Eu^{3+}

Examples of Corrosion Reactions:

$$\mathrm{M}^0 + x\mathrm{HF} \rightleftarrows \mathrm{MF}_x + \frac{x}{2}\mathrm{H}_2$$

$$\mathrm{Cr} + \mathrm{FeF}_2 \rightleftarrows \mathrm{CrF}_2 + \mathrm{Fe}$$

Salt Purification Methods

- Thermal purification to remove moisture
- Physical purification to remove gaseous species
  - Inert gas purging, vacuum, physical removal of deposits
- Chemical purification to remove non-gaseous species (oxides)
  - HF/H_2 for fluorides, HCl/H_2 for chlorides
  - Reactive metals (normally, select the metal whose potential is highest among the salt components, for example, Mg for $MgCl_2$-KCl-NaCl)
- Electro-chemical purification to remove metal halides

Purification Procedure

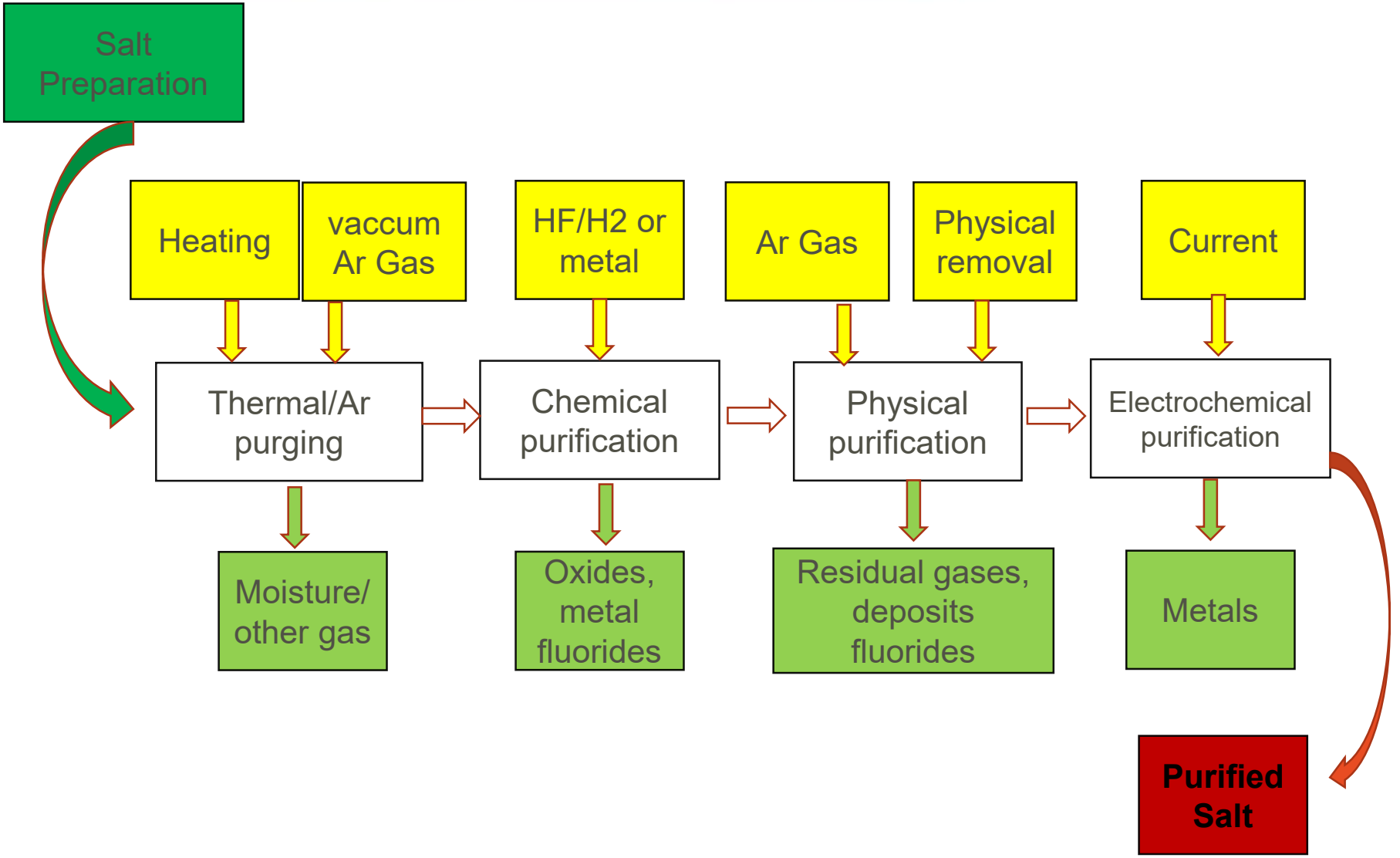

Analysis on impurities in salt

- Concentrations of oxygen and hydrogen in salts were measured using combustion analysis, showing the decrease of O and H concentrations.
- The Ni concentration was reduced after CA.

- O/H analysis on as-received NaF, KF, and UF_4 and thermally and chemically purified FUNaK

Salt	Concentration, µg/g	
	O	H
NaF	1608.26 ± 27.13	174.29 ± 8.15
KF	876.93 ± 94.10	48.92 ± 14.16
UF_4	1757.56 ± 156.28	37.02 ± 6.91
Chemically purified FUNaK	312.03 ± 123.85	15.12 ± 8.15
Thermally purified FUNaK	1593.31 ± 425.18	13.98 ± 5.11

- ICP-MS analysis before and after CA

Sample	Concentration, mol%			
	Cr	Mn	Fe	Ni
Pre-test	0.004 ± 0.002	0.001 ± 0.000	0.034 ± 0.007	0.173 ± 0.010
Post-test	0.000 ± 0.000	0.000 ± 0.000	0.005 ± 0.001	0.016 ± 0.006
Change	-0.004	-0.001	-0.029	-0.157

FeF_2 and NiF_2 were reduced by H_2, but not CrF_2

- Around 350 g of FUNaK was purged by Ar-20%H_2 gas for 8 hours at 600 °C.
- Metal particles were observed mostly at the bottom of the salt, and some of them were on its side and surface.
- The SEM/EDS mapping analysis indicates that the particles consist of Fe and Ni which might be from the reduction of FeF_2 and NiF_2 introduced from SS316L tubes and Ni lid of the system.
- CrF_2 in the salt was not reduced by H_2.

Top and side views

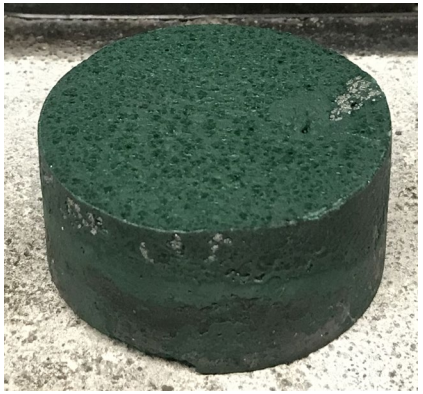

Bottom view

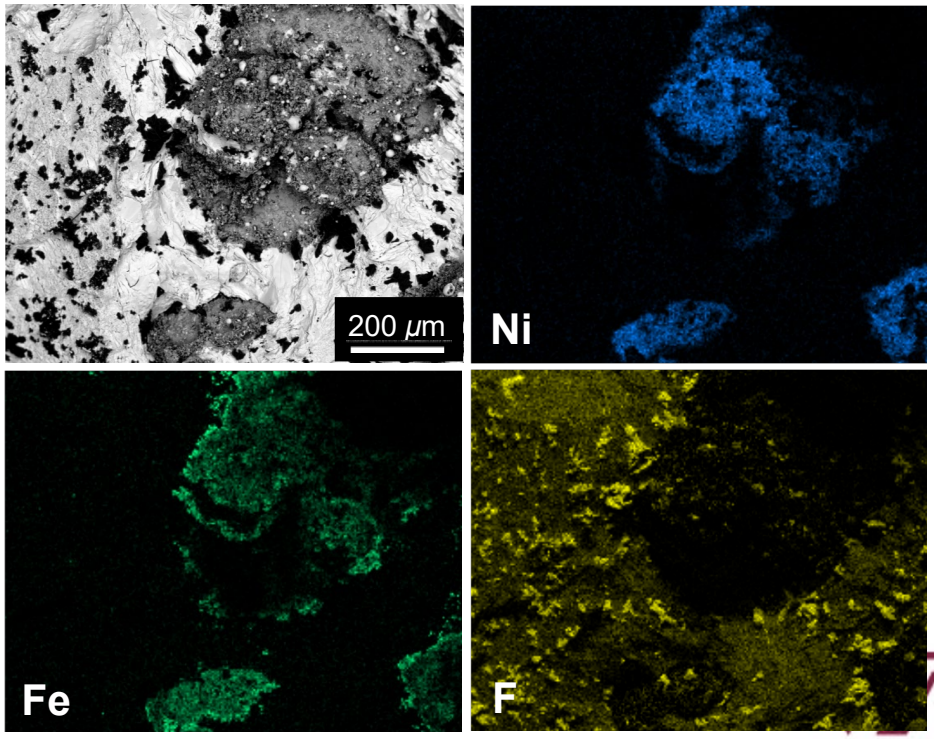

Ni and other metal impurities were removed using CA

- Thin Ni tube was immersed in molten salt during the gas purging, and some Ni was introduced to salt as NiF_2.
- Metallic impurities were reduced by performing chromoamperometry (CA).
- NiF_2 was reduced to Ni metal that was observed on the surface of salt and on the working electrode after CA.

Chronoamperometry setup

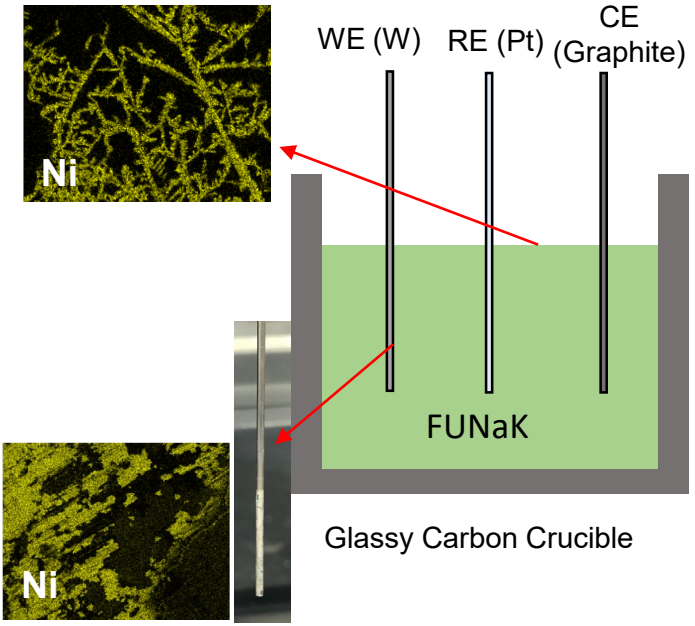

After 0.2 hours of CA

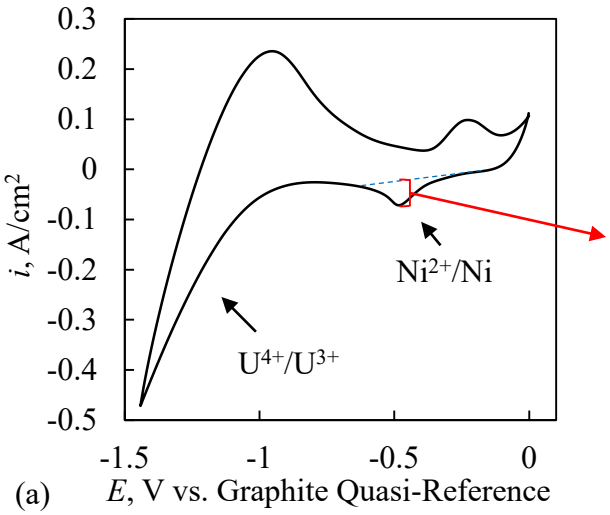

Peak heights change

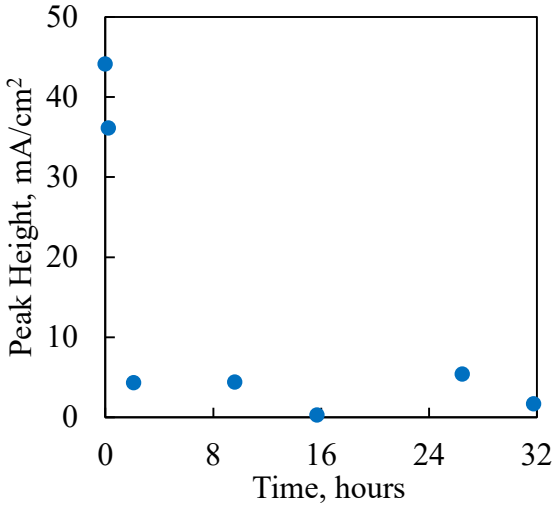

VIRGINIA TECH

Static Corrosion Test Setup

- Mainly two different batches of FUNaK were prepared: thermally purified and chemically purified (HF+CA) salts.
- For the chemically purified FUNaK, two different batches with and without UF_3 were prepared to study the impact of UF_3 on corrosion.
- Experiment Conditions: 800 °C for 120 hours. The same ratio of salt mass to specimen's surface area was used between tests with thermally and chemically purified salts.

With thermally purified salt

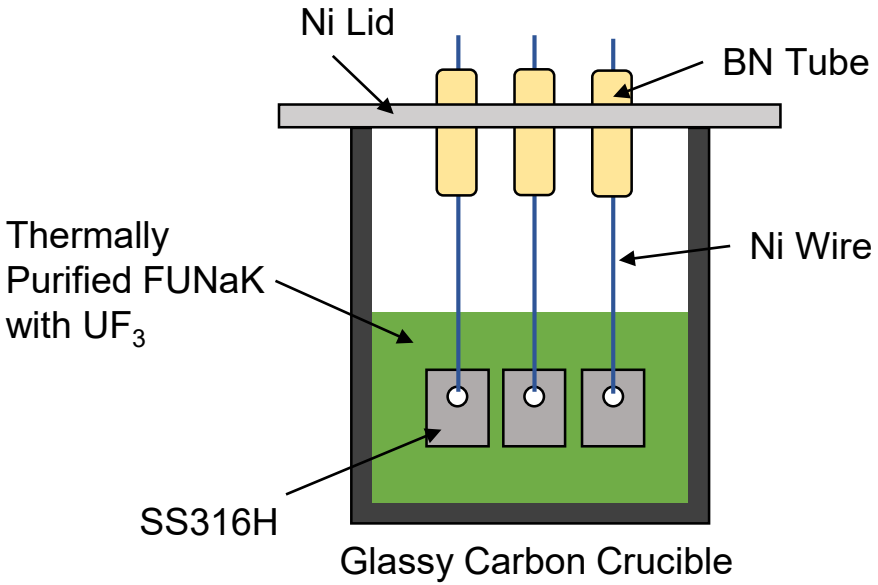

With chemically purified salts

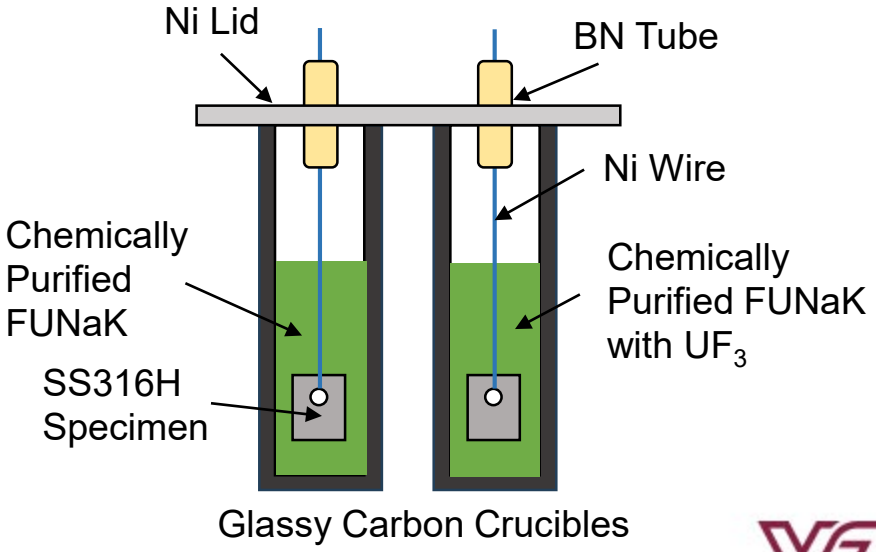

Flow-Induced Corrosion Test Setup

- Two different batches of FUNaK were prepared for 2 m/s dynamic corrosion tests: Thermally purified FUNaK with UF_3 and chemically purified FUNaK
- Hollow cylinder-shaped SS316H specimens were fixed between cylindrical boron nitride (BN) insulators and rotated in molten salt to simulate the flow of molten salt (Test conditions: 800 °C for 120 hours).
- Salt samples were intermittently collected during the tests to investigate concentration changes of corrosion products.

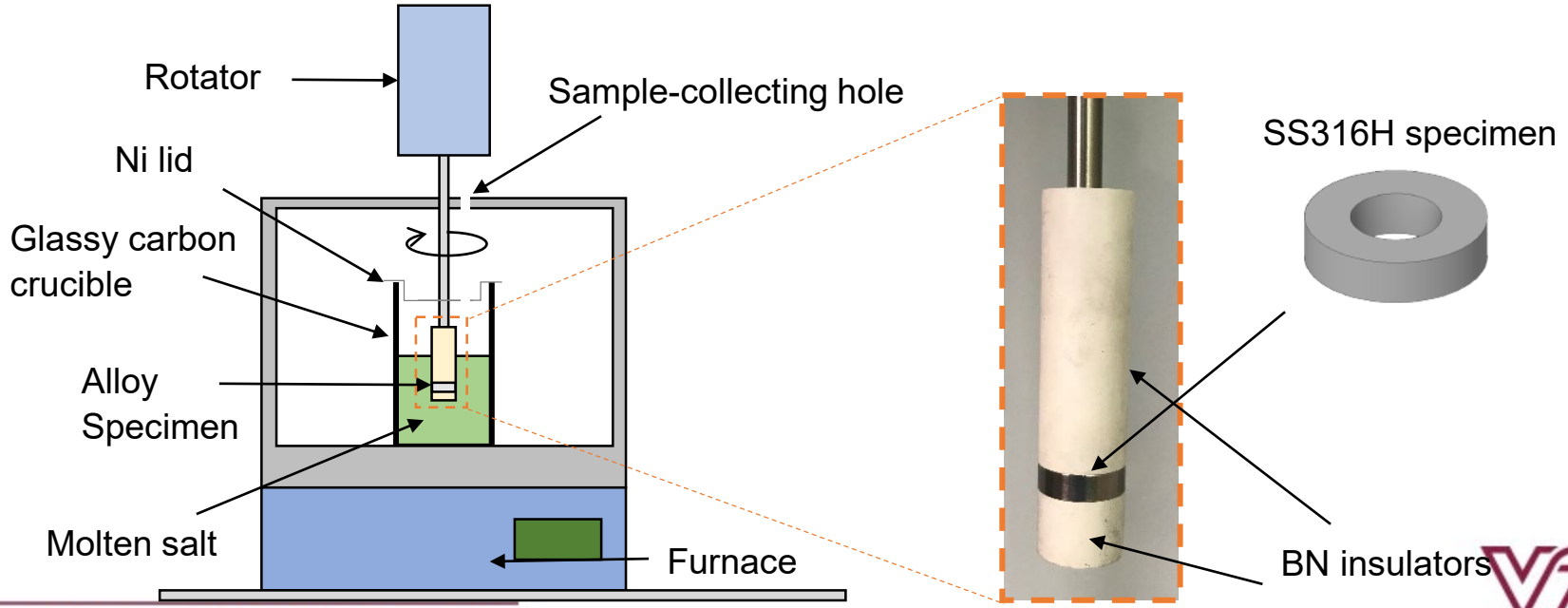

Chemical purification of FUNaK mitigated corrosion of SS316H

- Severe salt penetration through grain boundaries was observed from SS316H corroded by thermally purified salt.
- Compared to SS316H corroded by thermally purified FUNaK, those corroded by chemically purified salts showed much less corrosion with smaller salt-attack depth.

Corroded by **thermally** purified salt [5]

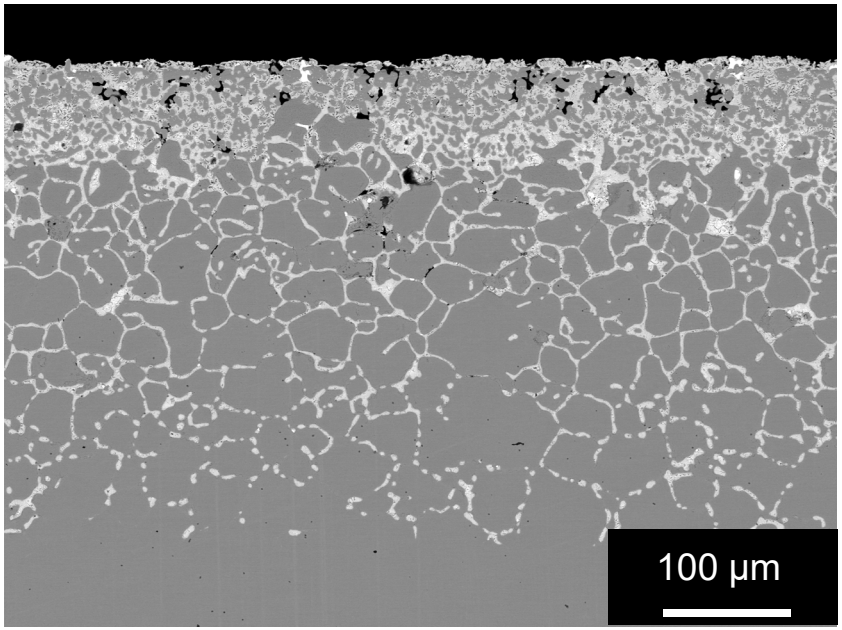

Maximum Salt-attack Depth: 504.14 µm

Corroded by **chemically** purified salt

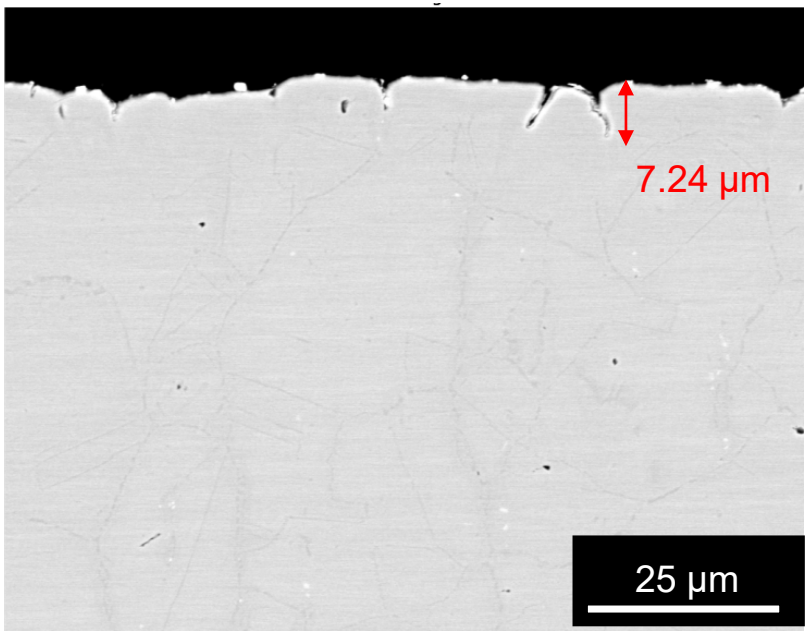

Maximum Salt-attack Depth: 7.24 µm

[5] Q. Yang, Kinetic Property and SS 316/Alloy 617 Corrosion Study in Molten Chloride and Fluoride Salts, Virginia Tech, 2022

Cr depletion occurred along grain boundaries

- Cr depletion was observed on grain boundaries near the surface of the SS316H specimen corroded by chemically purified salts.
- The segregation of Cr and Mo on grain boundaries were observed in the bulk of the specimen.
- Fe concentration increased on the surface of post-test SS316H indicating the reaction between FeF_2 and Cr: $FeF_2 + Cr \rightleftarrows Fe + CrF_2$.

BSE Image and EDS Mapping on cross section near the surface of post-test SS316H

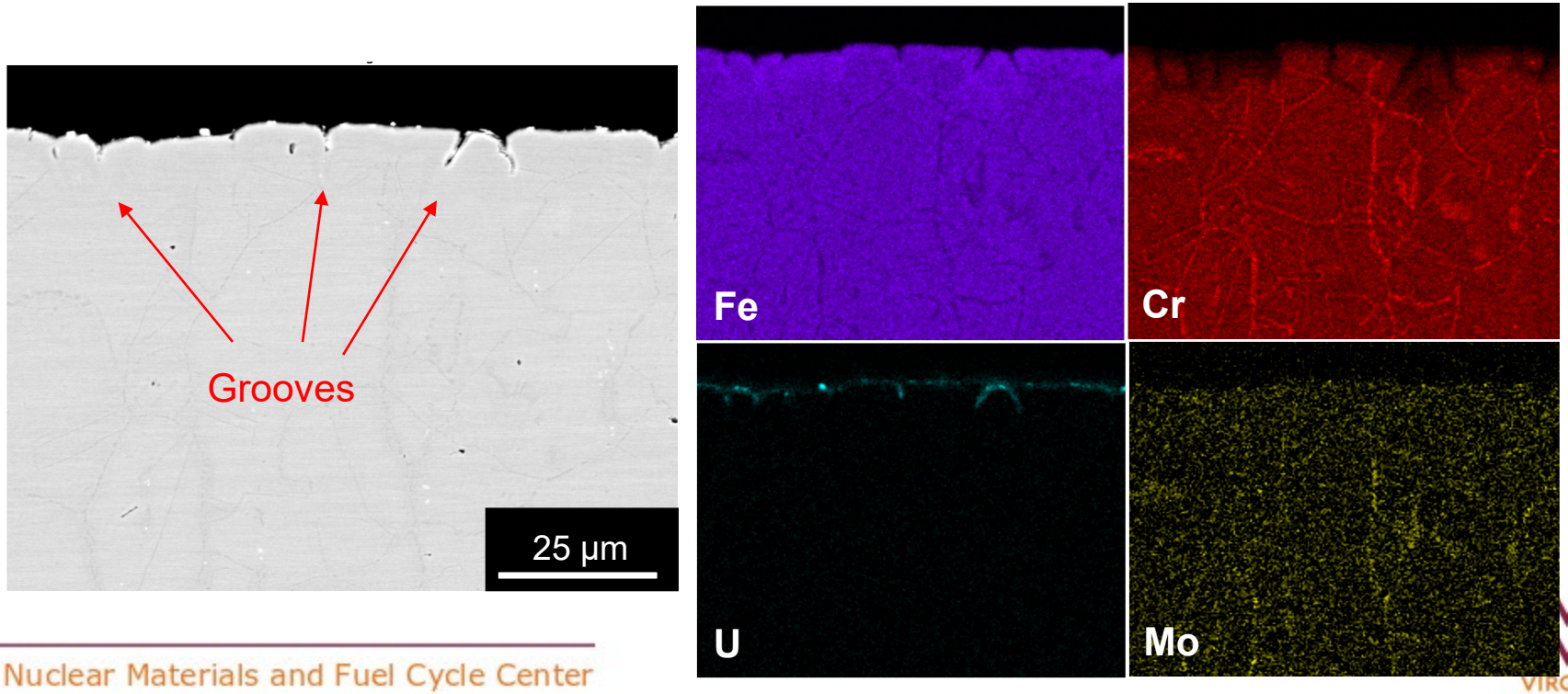

Presence of UF_3 did not show any meaningful differences

- Maximum Cr-depletion depths of post-test SS316H corroded by chemically purified FUNaK with and without UF_3 are 16.46 and 16.74 μm, respectively.

BSE Image and Cr EDS Mapping of post-test SS316H corroded by chemically purified salts

Corroded by chemically purified FUNaK + UF_3

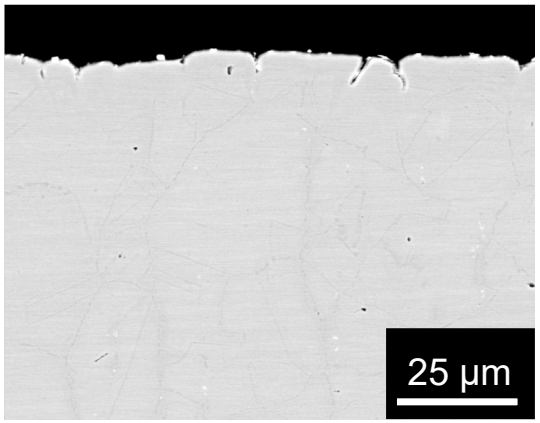

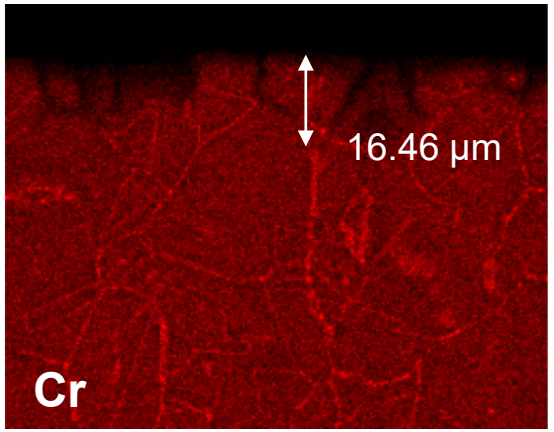

Corroded by chemically purified FUNaK

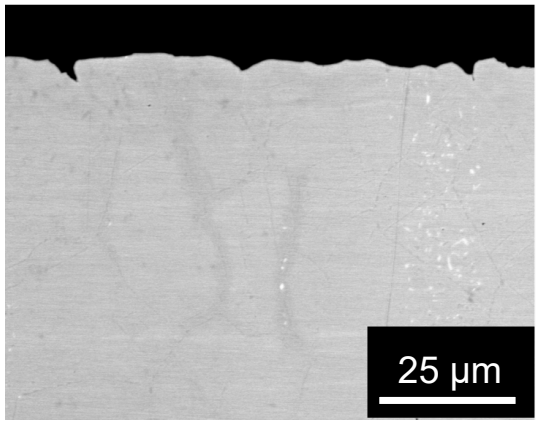

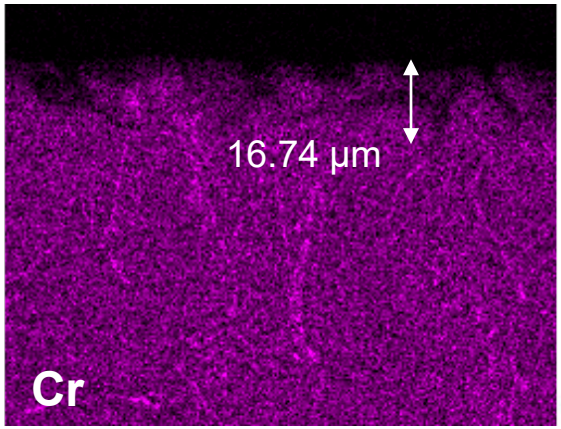

Sigma grain boundaries were observed in post-test specimen

- Many twin grain boundaries (Σ grain boundaries) were observed in the post-test specimen.
- Although some twin boundaries were observed from pre-test SS316H, the number of them increased possibly due to the annealing effect during the cooling process

- BSE Image and EDS Mapping of Σ GBs in Post-test SS316H corroded by chemically purified salts.

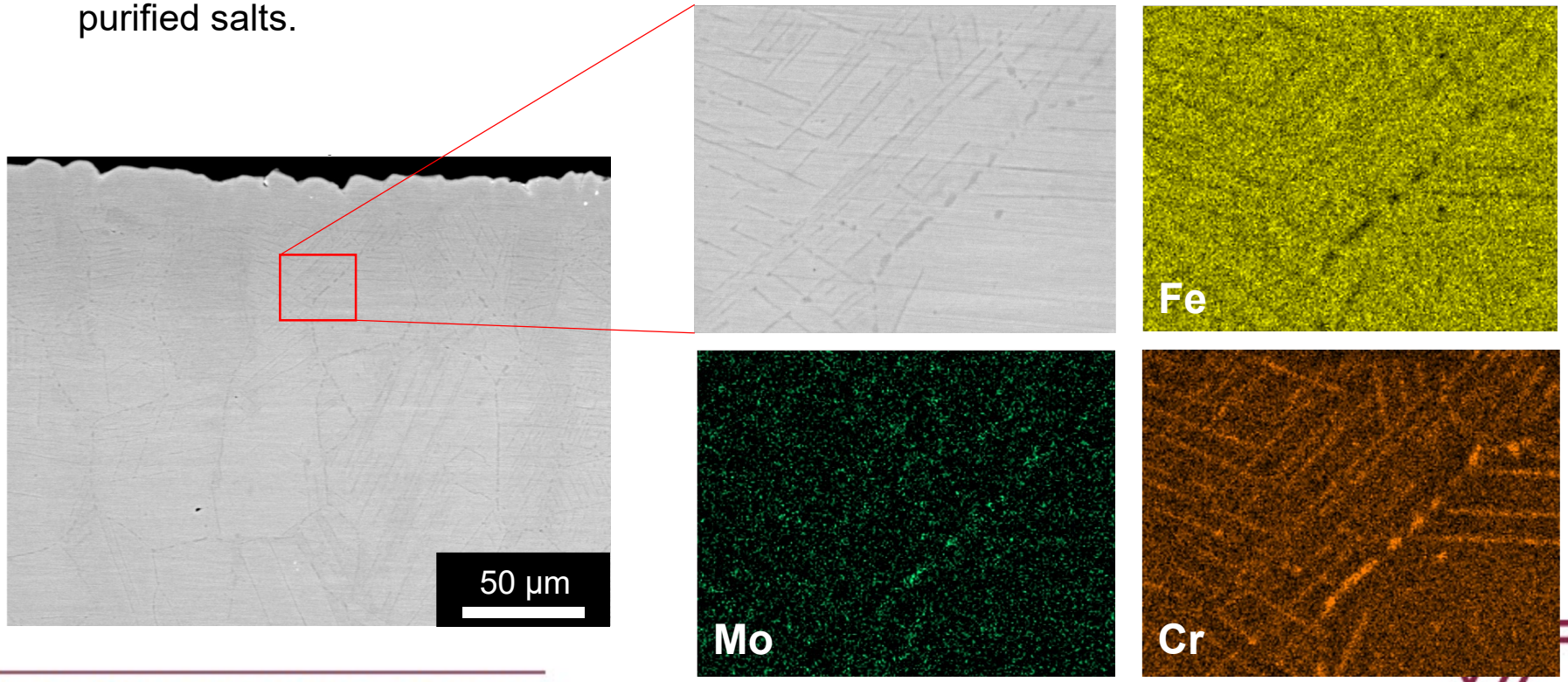

Grooves were formed along grain boundaries on surface

- The surface analysis on post-test SS316H showed the formation of grooves along its grain boundaries.
- The line-scan analysis across the grooves showed higher concentrations of Cr and Mo near grain boundaries, which indicates their segregation toward grain boundaries.
- Fe concentration in grooves is higher than other area indicates the reduction of dissolved FeF_2 and oxidation of Cr at grain boundaries.

BSE image and line-scan analysis across grooves on the surface of post-test SS316H

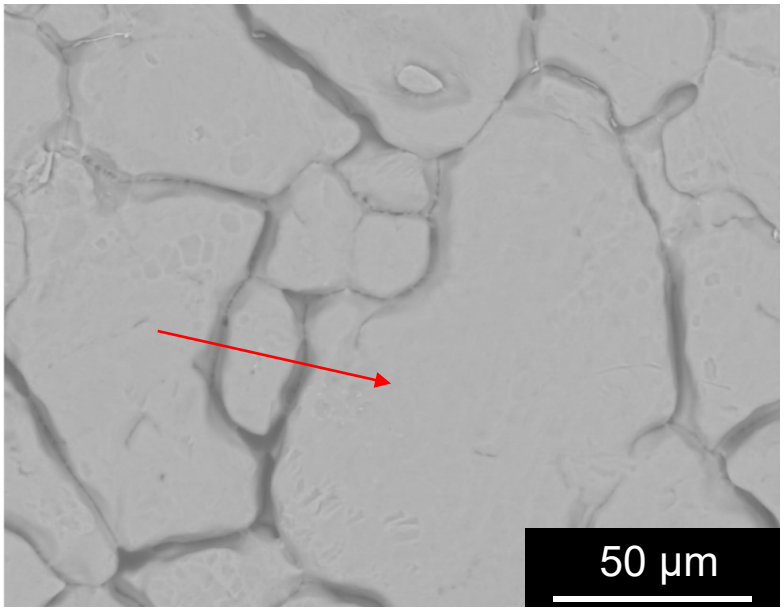

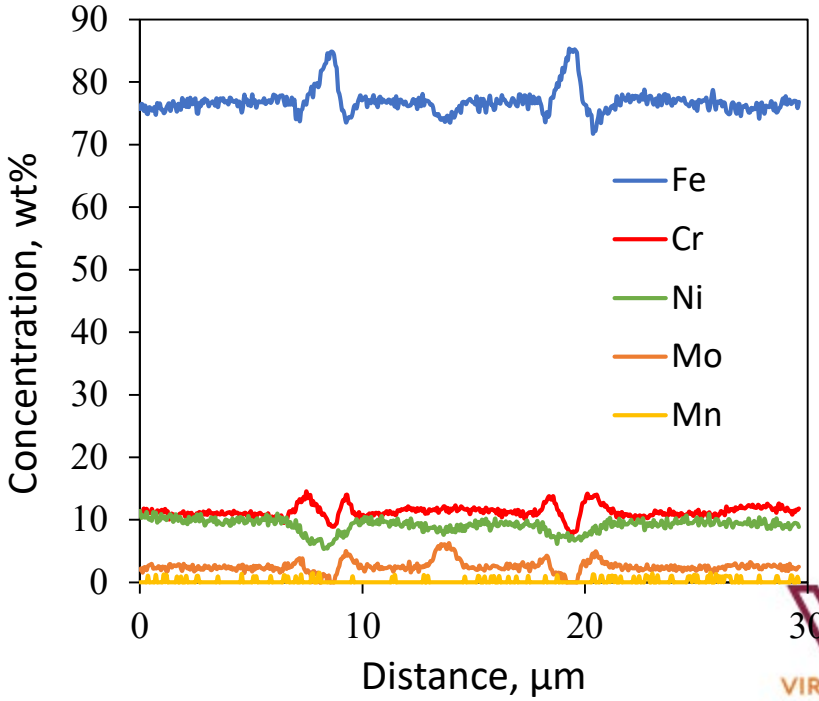

Mo diffused out on attacked grain boundaries

- Mo enrichment was observed in grooves on the surface of the SS316H corroded by chemically purified salts.

BSE image and Mo EDS mapping analysis for the surface of the post-test SS316H

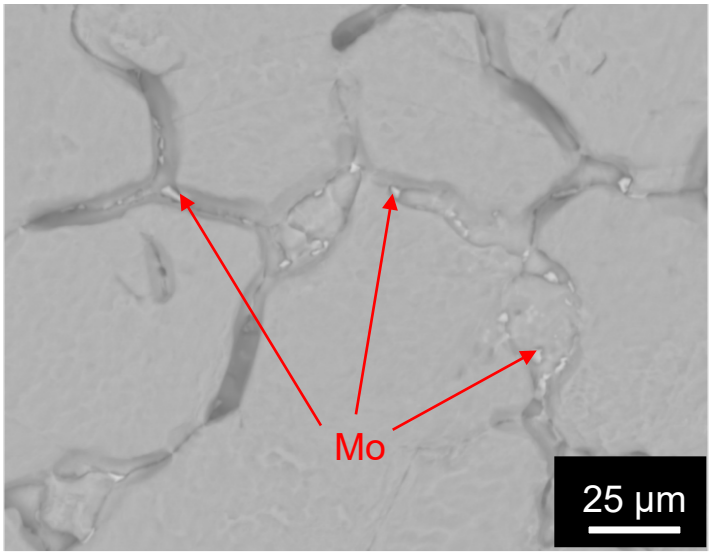

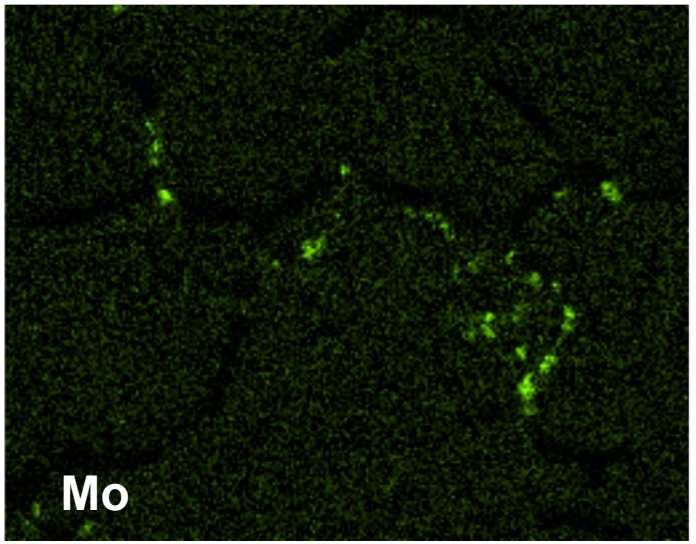

Dynamic corrosion test also showed importance of purification

- The surface of SS316H corroded by thermally purified salt became uneven, and massive salt attack was observed from the cross-sectional analysis.
- Voids and cracks were formed in the complete Cr-depleted area of SS316H corroded by thermally purified salt.
- Compared to the test using thermally purified salt, SS316H corroded by chemically purified salt showed much less salt penetration.

Post-test SS316H Specimen

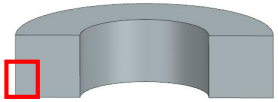

Corroded by **thermally** purified salt

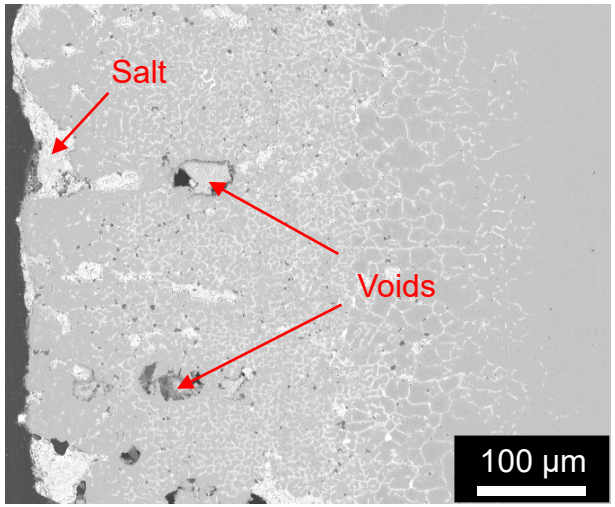

Corroded by **chemically** purified salt

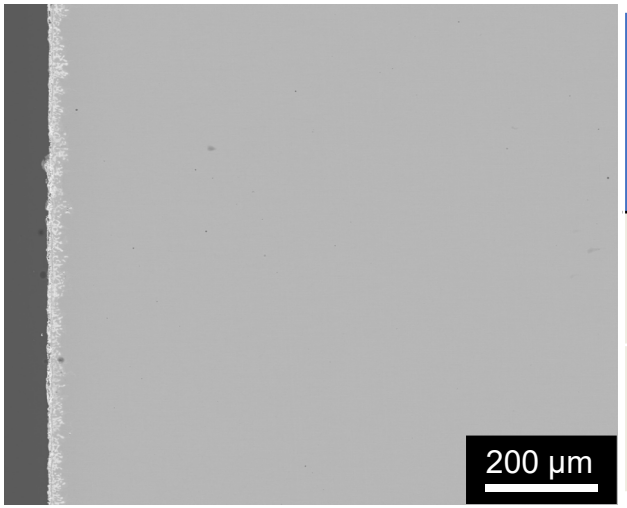

Salt-attack depths

Salt	Corrosion Depth, mm
Thermally purified	0.766 ± 0.021
Chemically purified	0.020 ± 0.008

Chemical purification reduced corrosion products in salt

- The dissolution of corrosion products was reduced by chemically purifying salt.
- For the thermally purified salt, the dissolution of Fe and Cr increased rapidly as the test started.
- The Fe concentration then decreased while the Cr concentration gradually increased due to the reaction between FeF_2 and Cr and the formation of carbides on the glassy carbon crucible.

Concentration changes of Fe and Cr in thermally and chemically purified salts during tests

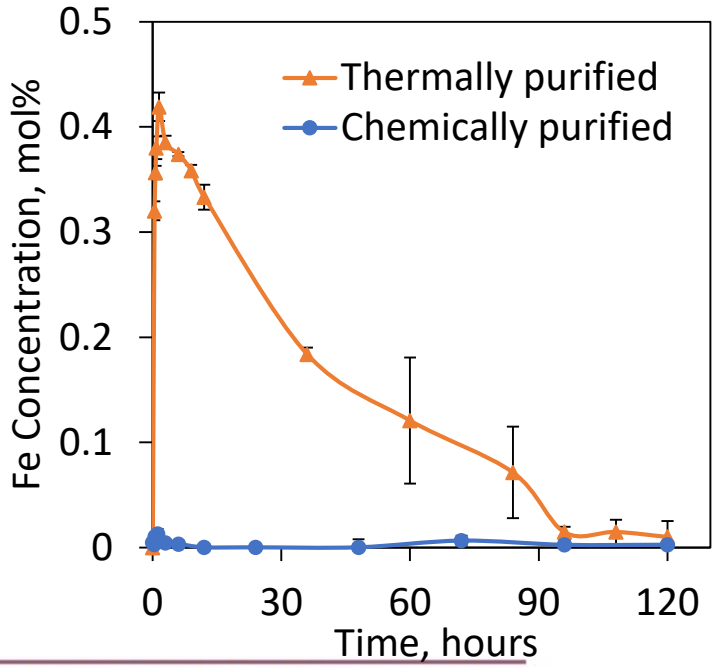

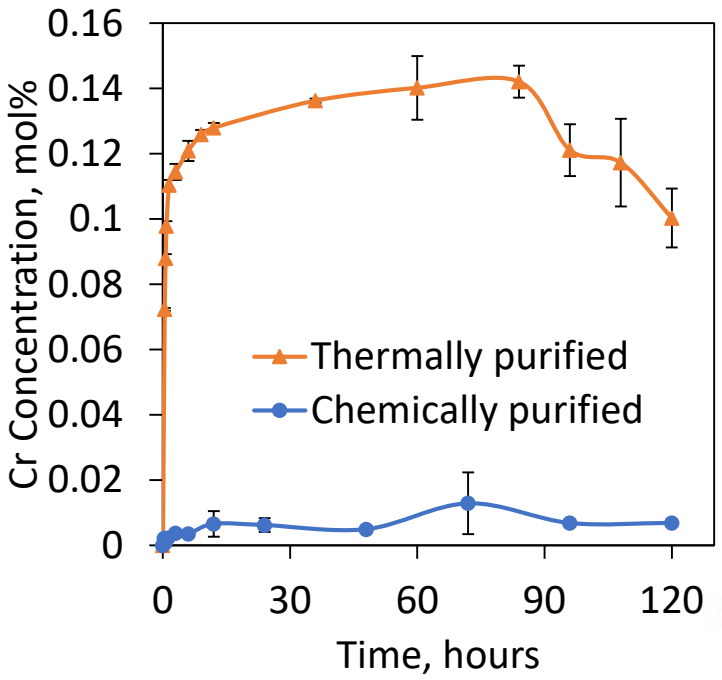

Silver-colored layers on post-test glassy carbon crucible

- Unlike the test using chemically purified salt, silver-colored layers were observed on the glassy carbon crucible after the test using thermally purified salt.
- The thickness of the layers was around 1.315 ± 0.707 μm.
- The post-test crucible from the 2 m/s test broke without significant force when it was being taken out of the furnace. This might be caused by the difference in thermal expansion between glassy carbon and materials of the layers.

Pre-test crucible

After the 2 m/s Test using **thermally** purified salt

BSE Image of layers' cross section

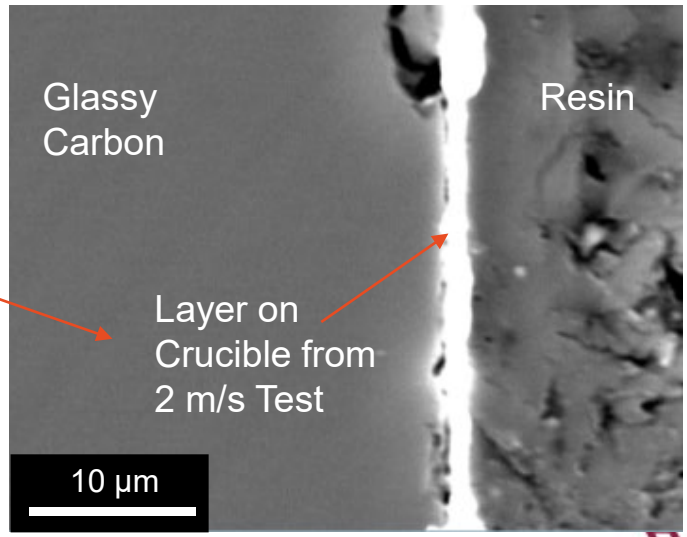

Layers mainly consist of $(Cr, Fe)_7C_3$.

- EDS mapping and XRD analyses showed that the layers on glassy carbon mainly consist of $(Cr, Fe)_7C_3$.
- This non-electric transfer of Cr and Fe occurred through the disproportionation reaction as reported by Ozeryanaya [6]:

$$3CrF_2 \rightleftarrows 2CrF_3 + Cr$$

- Following reactions are thermodynamically favorable:

$$7Cr + 3C \rightleftarrows Cr_7C_3$$
$$Cr_7C_3 + 7FeF_2 \rightleftarrows Fe_7C_3 + 7CrF_2$$

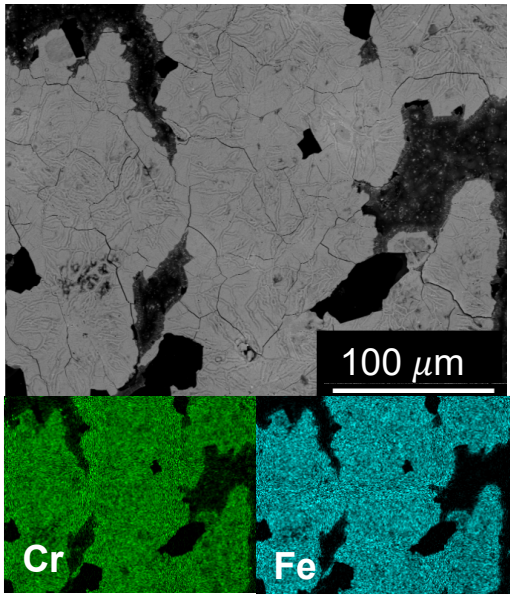

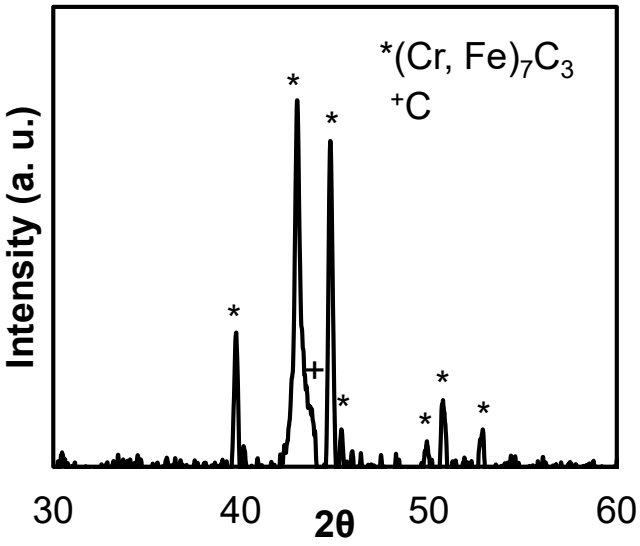

[6] Ozeryanaya, Corrosion of Metals by Molten Salts in Heat-treatment Processes, Met. Sci. Heat Treat. 27 (1985) 184–188.

Different structures were formed on the layers

- The dominant structure is (Cr, $Fe)_7C_3$ showing some dendritic morphology of its surface.
- Areas between (Cr, $Fe)_7C_3$ layers consist of Cr-metal particles and other dendritic structures as well as glassy carbon.

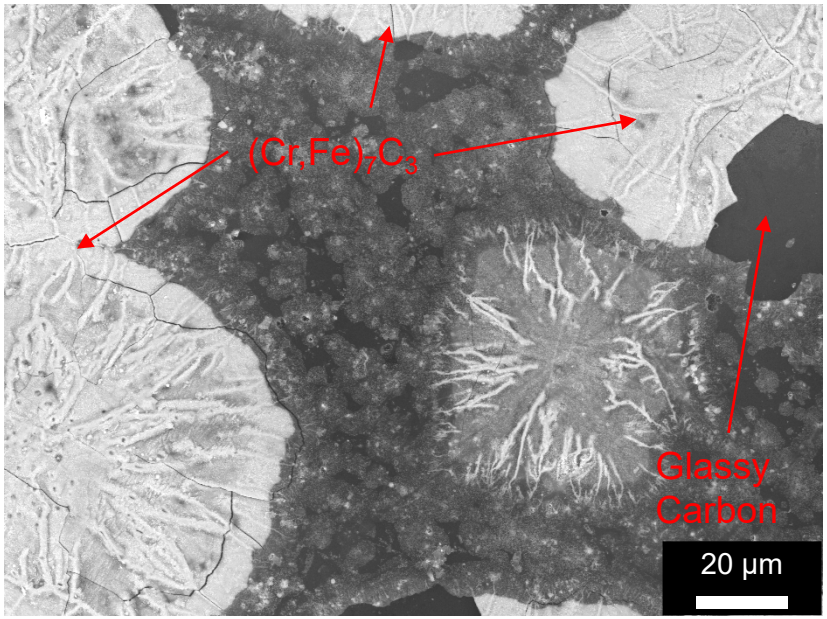

*BSE images were taken at an accelerating voltage of 20 kV, and the point scan was performed at 5 kV.

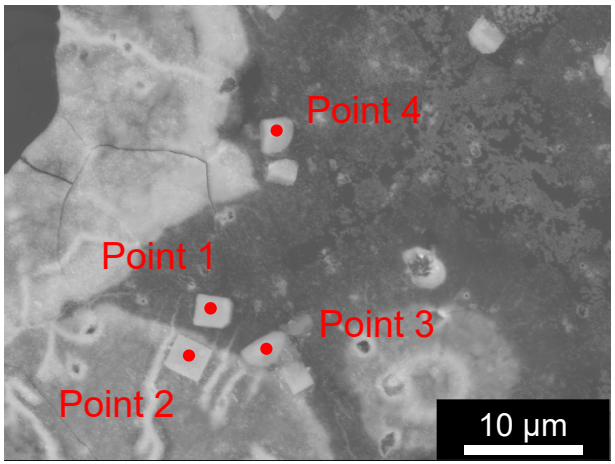

Point	Concentration, at.%	
	Cr	C
1	86.3	13.7
2	87.4	12.6
3	88.0	12.0
4	90.4	9.6
Average	88.0 ± 1.7	12.0 ± 1.7

Branches of dendritic structures with higher Cr and Fe

- The yellow arrow indicates the analysis line and direction of the line scan, and red arrows are intersections between the yellow arrow and branches of the dendritic structure.
- When the line scan was performed across the branches, concentrations of Cr and Fe increased while C concentration decreased.
- This dendritic structure might be the intermediate phase before forming the $(Fe, Cr)_7C_3$ layers.

BSE Image of a dendritic structure

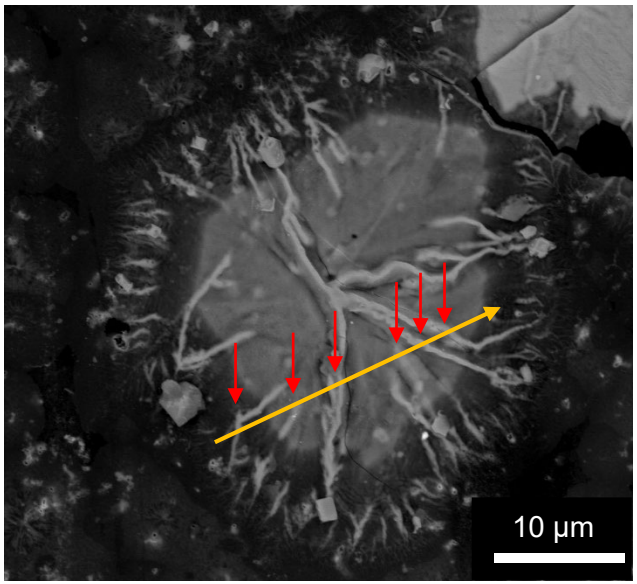

Line-Scan results along the yellow arrow

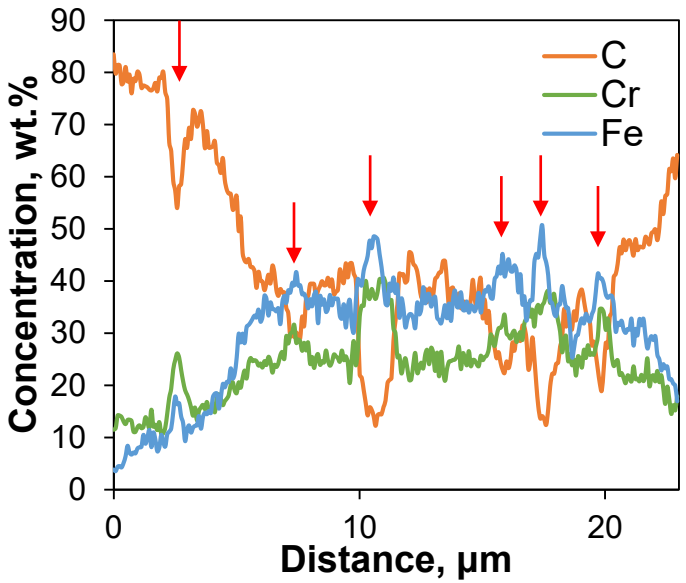

VIRGINIA TECH

U compounds were observed on carbide layers

- Small U-concentrated particles were found on $(Cr, Fe)_7C_3$ layers, which can be uranium oxides and/or uranium carbides.
- Uranium oxides are possibly from the salt.
- The formation of uranium carbides are possibly from the reaction between UF_3 and glassy carbon [7]:

$$4UF_3 + xC \rightleftarrows UC_x + 3UF_4$$

BSE Image of Carbide Layers

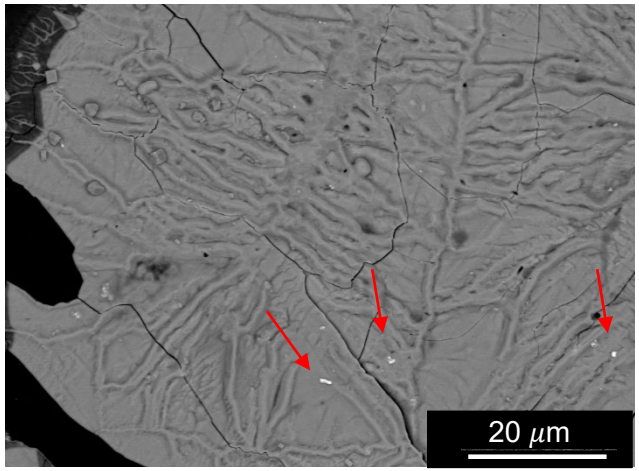

*Accelerating Voltage: 20 kV

SE Image of a U-concentrated Particle

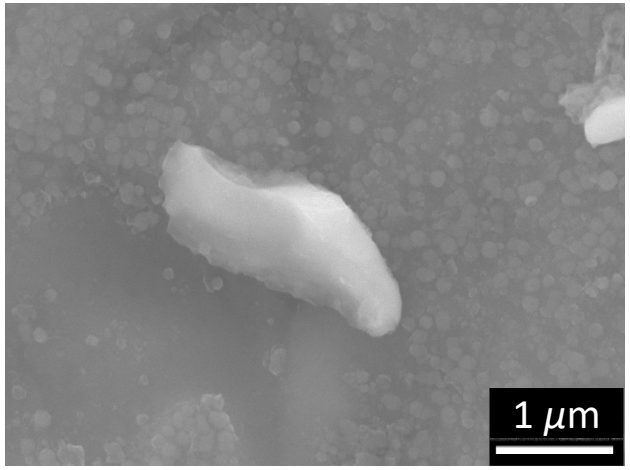

*Accelerating Voltage: 20 kV

Point-scan Results

Element	Concentration, at.%
U	21.3 ± 3.7
C	46.7 ± 3.1
O	22.2 ± 8.5
Cr	5.0 ± 2.2
Fe	4.8 ± 2.1

*Accelerating Voltage: 10 kV

[7] Toth and Gilpatrick, The Equilibrium of Dilute UF_3 Solutions Contained in Graphite, Oak Ridge, Tennessee, 1972.

Pitting corrosion on SS316H corroded by chemically purified salt

- The depletion of Cr and Mn was still observed near the surface.
- Cr-concentrated spots were observed near salt attack, and their number density became lower as being further from the surface. This might be caused by the accelerated diffusion of Cr by the gradient of its concentration.
- Layers concentrated with Fe and Ni were formed on the surface of SS316H during the test indicating the reduction of dissolved FeF_2 and NiF_2 to Fe and Ni and the acceleration of Cr and Mn dissolution.

- BSE Images and EDS mapping data of SS316H corroded by chemically purified FUNaK

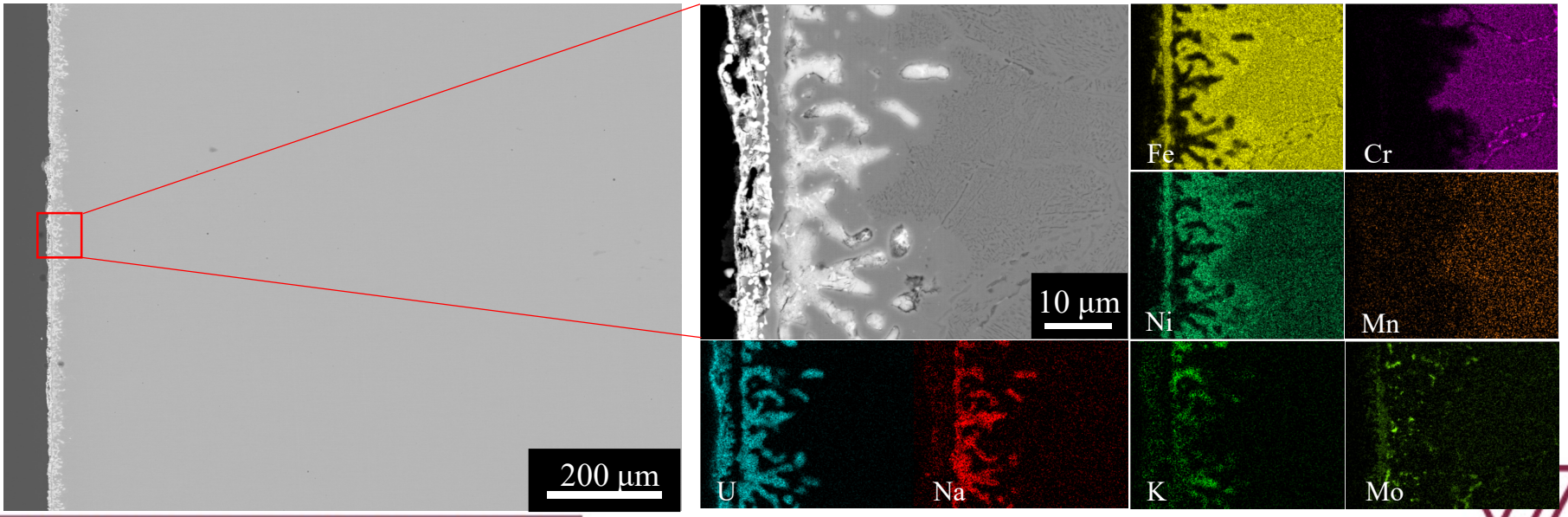

Pitting corrosion occurred on the surface of SS316H

- SS316H corroded by chemically purified FUNaK showed pitting corrosion on its surface after ultrasonic cleaning in DI water.
- The Fe and Ni concentrated layers on the surface observed from the cross-sectional analysis might be removed during the ultrasonic cleaning.
- The diameters of pits are aligned with the width of salt attacks observed from the cross-sectional analysis.

  - BSE Images for the surface of SS316H corroded by chemically purified FUNaK

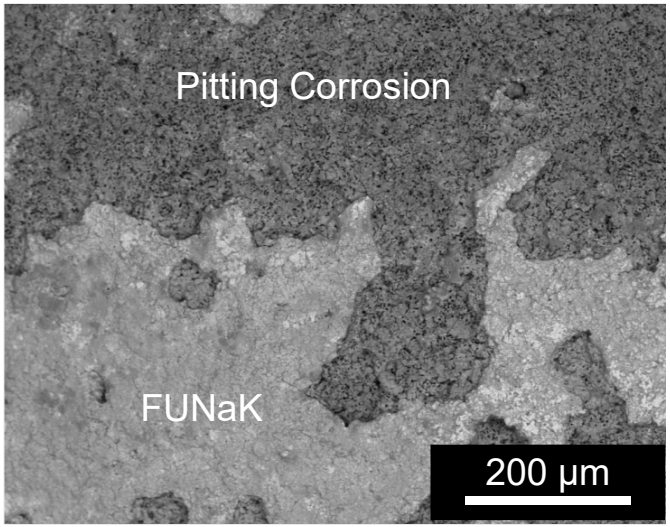

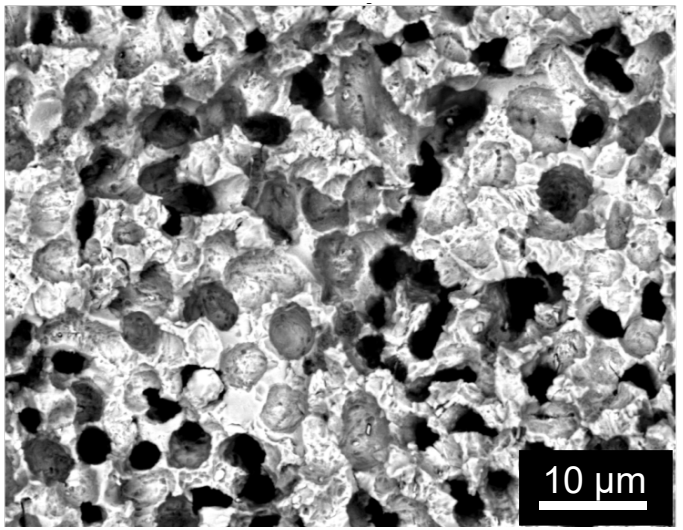

Chemical purification of salt reduces corrosion of SS316H

- HF, moisture, oxides, and metallic impurities are main contaminants that cause the corrosion of structural alloys for molten salt reactors.
- Oxides, hydroxides, and sulfides can be removed with hydrofluorination, and metallic impurities can be removed with chronoamperometry.
- Static and dynamic corrosion tests showed that chemical purification (hydrofluorination + chronoamperometry) of salt mitigated the corrosion of SS316H significantly.
- The dissolution of metallic components in SS316H mainly occurred from its grain boundaries.
- Cr and Mo diffuse from grains to grain boundaries during the corrosion of SS316H, and the reaction between dissolved FeF_2 and Cr of SS316H occurs at the interface between salt and SS316H, especially grain boundaries near the interface.
- Interactions between corrosion products (CrF_2 and FeF_2) and glassy carbon caused the formation of (Fe, $Cr)_7C_3$ layers, Cr-metal particles, and other dendritic structures concentrated with Fe and Cr.

Acknowledgement

- The authors would like to acknowledge Dr. Qiufeng Yang for conducting the static corrosion tests of SS316H using thermally purified FUNaK with UF_3.
- The authors would like to thank Dr. Amanda Leong for invaluable advice on this research.